Accepted Manuscript

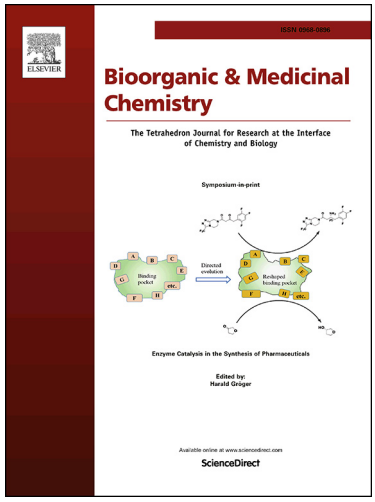

Design, Synthesis, Biological Activities, and Dynamic Simulation Study of Novel Thiourea Derivatives with Gibberellin Activity towards *Arabidopsis thaliana*

Zhikun Yang, Jine Wang, Hao Tian, Yan He, Hongxia Duan, Liusheng Duan, Weiming Tan

PII: S0968-0896(19)30402-X
DOI: https://doi.org/10.1016/j.bmc.2019.06.032
Reference: BMC 14969

To appear in: *Bioorganic & Medicinal Chemistry*

Received Date: 11 March 2019
Revised Date: 9 June 2019
Accepted Date: 19 June 2019

Please cite this article as: Yang, Z., Wang, J., Tian, H., He, Y., Duan, H., Duan, L., Tan, W., Design, Synthesis, Biological Activities, and Dynamic Simulation Study of Novel Thiourea Derivatives with Gibberellin Activity towards *Arabidopsis thaliana*, *Bioorganic & Medicinal Chemistry* (2019), doi: https://doi.org/10.1016/j.bmc.2019.06.032

Design, Synthesis, Biological Activities, and Dynamic Simulation Study of Novel Thiourea Derivatives with Gibberellin Activity towards *Arabidopsis thaliana*

Zhikun Yang[a, 1], Jine Wang[a, 1], Hao Tian[a], Yan He[a], Hongxia Duan[b], Liusheng Duan[a], Weiming Tan[a*]

[a] College of Agronomy and Biotechnology, China Agricultural University, Beijing, 100193, P. R. China

[b] Department of Applied Chemistry, China Agricultural University, Beijing, 100193, P. R. China

Abbreviations:

* Corresponding author.

E-mail address: tanwm@cau.edu.cn (W. M. Tan)

[1] These authors contributed equally.

ABSTRACT

Computer-aided drug design has advanced by leaps and bounds, and has been widely used in various fields, and especially in the field of drug discovery. Although the crystal structure of the gibberellin (GA) receptor GID1A had been reported in previous studies, there is still a lack of designs of gibberellin functional analogue

based GID1A. In the present study, a series of 30 thiourea derivatives were designed, synthesized and biologically assayed. The results suggested that the synthetic compounds had good GA-like activities. Furthermore, the structure-activity relationship of the synthetic compounds was discussed, and the dynamic simulation and docking study revealed the binding properties of the GID1A receptor and compounds Y1, Y11, and Y21.

Keywords: GID1A receptor; Gibberellin activity; Thiourea derivatives; Arabidopsis

1. Introduction

Plant hormones are widespread in nature and play an important regulatory role in growth and development as an indispensable signal substance in plants.[1] Gibberellins (GAs) are an important group of isoprenoid phytohormones that occur in minute amounts. In 1938, the GA_3 crystal was firstly extracted from the Gibberella causing rice seedling disease. In 1958, MacMillan purified gibberellin (GA_1) from immature bean seeds, and since then, more than 130 GAs have been identified.[2] Gibberellins, found in higher plants, algae, fungi, and bacteria, are widely used as plant growth regulators of many developmental processes, such as root and shoot elongation, dormancy break, promotion of seed germination, leaf stretching, and flower regulation in agricultural production, including flower preservation, and beer brewing.[3-5] However, GAs are a class of tetracyclic diterpenoid hormones (Fig. 1), which have 136 different complex structures. From these structures, only a few, such as GA_1, GA_3, GA_4, and GA_7, are bioactive, which poses a rather more formidable challenge to organic synthesis and qualitative and quantitative analysis based on chromatographic techniques.[6,7] It can be seen that the discovery of a novel molecule with GA bioactivities is of enormous significance to the study of GA signaling mechanisms and practical applications.

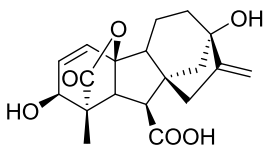

GA_3

pIC_{50}=5.30

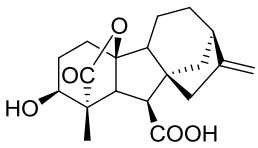

GA_4

pIC_{50}=7.30

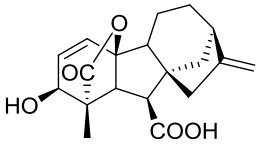

GA_7

pIC_{50}=7.30

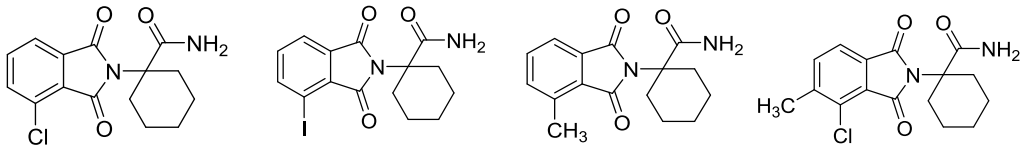

AC94377 AC006 AC007 AC015

pIC_{50}=4.24 pIC_{50}=4.12 pIC_{50}=4.40 pIC_{50}=4.47

Fig. 1. Chemical structure of gibberellic acids (GA_3, GA_4, GA_7) and the reported N-substituted phthalimide functional analogues.

In the past two decades, most studies were focused on GA receptors, with further research being focused on the mechanism of GA action, which revealed the GA signal transduction mechanism. In 2005, Ueguchi-Tanaka et al. cloned and encoded GA-related genes in rice, and discovered that GIBBERELLIN INSENSITIVE DWARF1 (GID1A) is a GA receptor, which was subsequently verified by Nakajim et al., who identified and characterized Arabidopsis gibberellin receptors.[8,9] In 2008, Murase et al. and Shimada et al. reported the crystal structure of GID1A-GA-DELLA complexes in Arabidopsis and rice, respectively.[10,11] It was found that GID1A-GA_3-DELLA was formed in plants and degraded after GA_3 was recognized by the GID1A protein, which caused the gibberellin effect and promoted hypocotyl elongation. These studies have provided a biological basis for the design of novel target-specific GA functional analogs. Until today, only one gibberellin functional analogue, named AC-94377, has been reported by the American Cyanamid Corporation in 1977.[12] It is a phthalimide-like substance that can break seed dormancy, stimulate hypocotyl elongation, and be recognized by GID1A in plants to form the

*At*GID1A-AC94377-DELLA complex, inducing the degradation of DELLA protein, similar to the action mechanism of GA_3. [13,14]

Nowadays, structure-based drug design based on receptor modeling has been widely applied in the research and discovery of new drugs, benefited from the rapid growth of computing power and the current level of theories and algorithms for studying macromolecular systems.[15,16] In addition, the screening technology plays an increasingly important role in drug design with its highly efficiency, fast, low cost, and high selectivity.[17] For example, the discovery of Indinavir based on HIV-1 protease, and the E2020 drug development based on acetylcholinesterase have been achieved using this technology. [18,19] However, few studies have focused on the design of GA functional analogues with GA receptor protein GID1A as the target.

In the present study, 1-(2,3-dimethoxyphenethyl)-3-(3-(trifluoromethyl) phenyl)thiourea, named Y1 in the MayBridge Screening Collection, was screened using the SYBYL software based on the GID1A protein, and 30 compounds were designed based on the isostere principle and active group splicing. Then, 30 compounds were synthesized and characterized by ^{1}H-NMR, ^{13}C-NMR and high-resolution mass spectrometry (HRMS). At the same time, the biological activities of the synthetic compounds were assayed and analyzed on *Arabidopsis thaliana*, and the structure-activity relationship was calculated and discussed. Finally, the growth situation of gibberellin-deficient dwarf mutant *ga1-1*, dynamical analysis, and molecular docking were used to verify that the produced compounds have similar function as GA_3.

2. Experimental section

2.1. Chemicals and seeds

All solvents were purchased from Tongguang (Beijing, China). All reagents were purchased from J&K Chemicals, Beijing, China. The solvents were dried and purified according to standard procedures. All commercially available reagents were used without further purification. Column chromatography was conducted on a silica gel plug (200–300 mesh), and the reaction progress was monitored by thin-layer chromatography on silica gel GF-254 and detected under UV light.

The plant Arabidopsis (A. thaliana ecotype Columbia-0, Col-0) and its gibberellin-deficient mutant *ga1-1* were provided by the State Key Lab of Plant Physiology and Biochemistry, China Agricultural University, Beijing, China.

2.2. Instruments

Pharmacophore models were built using the GALAHAD module in the SYBYL 7.2 software, and multiple screening was performed by combining the Lipinski's rule of five, the pharmacophore model, and the Surflex-dock module. Dynamic simulation and binding free energy decomposition were generated using AMBER14. ^{1}H NMR and ^{13}C NMR spectra were obtained at 300 MHz using a Bruker AVANCE DPX300 spectrometer in $CDCl_3$ or DMSO-d_6 solution with tetramethylsilane as the internal standard. HRMS were performed using an Agilent 6520 Accurate-Mass-Q-TOF LC/MS system, equipped with an electrospray ionization (ESI) source in the positive ionization mode. The melting points were determined on a Stuart SMP3 melting point apparatus and were uncorrected. The *Arabidopsis* growth data was obtained using

ImageJ software (https://imagej.nih.gov/ij/index.html).

2.3 Pharmacophore models and virtual screening

Three gibberellins (GA_3, GA_4, GA_7) widely used in agricultural production and four N-substituted phthalimide (NSP) functional analogues (Fig. 1) that have higher than gibberellins activity and have a common target protein GID1A with gibberellin were used as training set to generate a 3D pharmacophore model using the GALAHAD module. Parameters including population size, max generations, mols required to N hit, and keep best N models were set to 45, 45, 5, and 20, respectively. In the end, twenty pharmacophore models were obtained and evaluated, and a representative model was selected based on the enrichment factor for virtual screening. Thiourea compounds were filtered out from the Maybridge database using the Lipinski's rule of five (M<450),[20,21] LogS (>-4), CLogP (<5), polar surface area (<120 $Å^2$), toxicity (irritant, tumorigenic, mutagenic, reproductive effective), physicochemical properties, pharmacophore model, and GID1A.

2.4. General Synthesis

The synthetic routes of all compounds are given in Fig. 2. In brief, a substituted aniline was employed to related aromatic isothiocyanate,[22] and followed by reaction with a substituted aromatic ethylamine to obtain a thiourea derivative, named Y1 to Y30, containing two aromatic rings.[23]

2.4.1. The preparation of aromatic isothiocyanate

Taking the synthesis of 3-(trifluoromethyl)phenyl 1-isothiocyanate as an example, 3-(trifluoromethyl)aniline (2.38 g, 14.77mmol, 1 eqv) and dimethylamino

thiocarbonyl chloride (1.92 g, 15.50 mmol, 1.05 eqv) were added in dry toluene (20 mL) at room temperature, and then the reaction mixture was refluxed for 5 h. After the reaction mixture was cooled down to room temperature, the solid dimethylamine hydrochloride was filtered off, and the collected toluene fraction was removed under reduced pressure. Colorless oil (2.55 g, 85%) was obtained and used in the next step without additional purification.

The other aromatic isothiocyanates were synthesized in the same way.

2.4.2. The preparation of thiourea derivatives

3-(trifluoromethyl)phenyl isothiocyanate (0.53 g, 2.60 mmol, 1 eqv) was dissolved in dichloromethane (30 mL), 2-(2,3-dimethoxyphenyl)ethyl amine (0.47 g, 2.60 mmol, 1 eqv) was added, and then the reaction mixture was stirred for 2 h. The solvent was evaporated off by vacuum, and subsequently the residue was recrystallized from ethylacetate. A white solid (0.92 g, 92 %) was obtained as compound Y1. m.p. 91.4-92.2°C. ^{1}H NMR (300 MHz, Chloroform-*d*) δ 8.69 (s, 1H), 7.48 – 7.36 (m, 3H), 7.27 (d, *J* = 7.3 Hz, 1H), 6.76 – 6.62 (m, 3H), 6.15 (s, 1H), 3.87 (q, *J* = 6.2 Hz, 2H), 3.81 (s, 3H), 3.78 (s, 3H), 2.86 (t, *J* = 6.7 Hz, 2H). ^{13}C NMR (75 MHz, $CDCl_3$) δ 180.05, 148.80, 147.48, 136.93, 131.84 (q, *J* = 33.0 Hz), 130.35, 130.03, 127.50, 122.78 (q, *J* = 7.2, 3.5 Hz), 122.49 (q, *J* =128.4 Hz), 120.95 (q, *J* = 3.8 Hz), 120.26, 55.48, 55.45, 45.86, 33.88. HRMS (ESI^-): m/z: 385.1189 $[M+H]^+$.

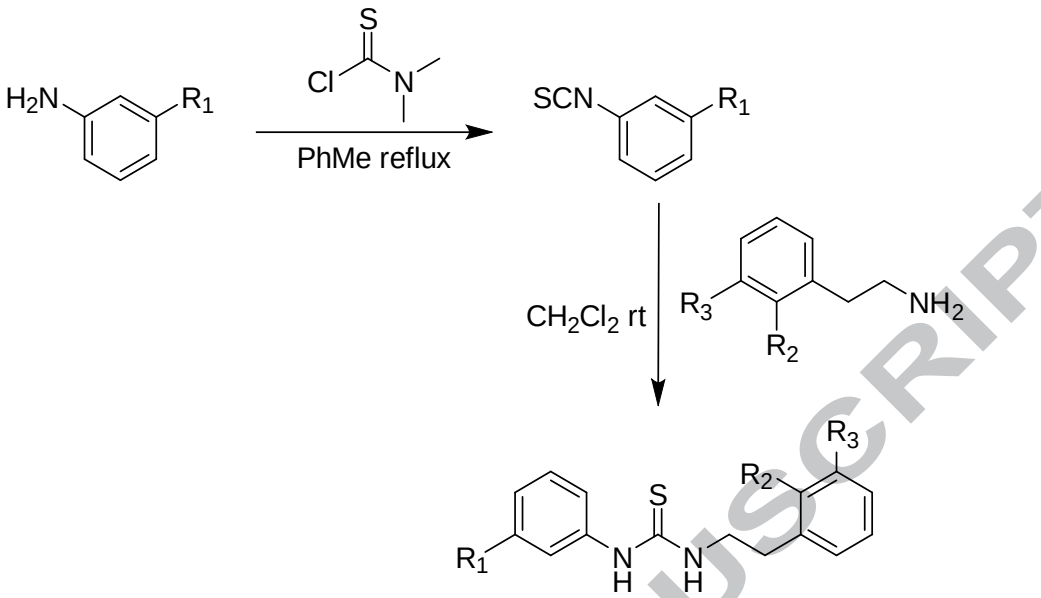

Y1: R_1=CF_3, R_2=OCH_3, R_3=OCH_3 Y11: R_1=CF_3, R_2=H, R_3=OCH_3 Y21: R_1=CF_3, R_2=H, R_3=H

Y2: R_1=CH_3, R_2=OCH_3, R_3=OCH_3 Y12: R_1=CH_3, R_2=H, R_3=OCH_3 Y22: R_1=CH_3, R_2=H, R_3=H

Y3: R_1=CH_2CH_3, R_2=OCH_3, R_3=OCH_3 Y13: R_1=CH_2CH_3, R_2=H, R_3=OCH_3 Y23: R_1=CH_2CH_3, R_2=H, R_3=H

Y4: R_1=$CH(CH_3)_2$, R_2=OCH_3, R_3=OCH_3 Y14: R_1=$CH(CH_3)_2$, R_2=H, R_3=OCH_3 Y24: R_1=$CH(CH_3)_2$, R_2=H, R_3=H

Y5: R_1=$C(CH_3)_3$, R_2=OCH_3, R_3=OCH_3 Y15: R_1=$C(CH_3)_3$, R_2=H, R_3=OCH_3 Y25: R_1=$C(CH_3)_3$, R_2=H, R_3=H_3

Y6: R_1=H, R_2=OCH_3, R_3=OCH_3 Y16: R_1=H, R_2=H, R_3=OCH_3 Y26: R_1=H, R_2=OH, R_3=H

Y7: R_1=F, R_2=OCH_3, R_3=OCH_3 Y17: R_1=F, R_2=H, R_3=OCH_3 Y 27: R_1=F, R_2=H, R_3=H

Y8: R_1=Cl, R_2=OCH_3, R_3=OCH_3 Y18: R_1=Cl, R_2=H, R_3=OCH_3 Y28: R_1=Cl, R_2=H, R_3=H

Y9: R_1=Br, R_2=OCH_3, R_3=OCH_3 Y19: R_1=Br, R_2=H, R_3=OCH_3 Y29: R_1=Br, R_2=H, R_3=H

Y10: R_1=I, R_2=OCH_3, R_3=OCH_3 Y20: R_1=I, R_2=H, R_3=OCH_3 Y30: R_1=I, R_2=H, R_3=H

Fig. 2. The synthetic routes of compounds Y1-Y30

3-(Trifluoromethyl)phenyl isothiocyanate (0.57 mg, 2.82 mmol, 1 eqv) was dissolved in dichloromethane (30 mL), 2-(3-methoxyphenyl)ethyl amine (0.43 mg, 2.82 mmol, 1 eqv) was added, and then the reaction mixture was stirred for 2 h. The

solvent was evaporated off by vacuum, and subsequently the residue was recrystallized from ethylacetate. A white solid (0.95 g, 95 %) was obtained as compound Y11. m.p. 59.8-61.0°C. ^{1}H NMR (300 MHz, Chloroform-*d*) δ 8.89 (s, 1H), 7.50 – 7.37 (m, 3H), 7.26 (d, *J* = 7.1 Hz, 1H), 7.21 – 7.14 (m, 1H), 6.81 – 6.64 (m, 3H), 6.16 (s, 1H), 3.87 (q, *J* = 6.5 Hz, 2H), 3.75 (s, 3H), 2.89 (t, *J* = 6.8 Hz, 2H). ^{13}C NMR (75 MHz, $CDCl_3$) δ 179.99, 159.59, 139.48, 136.83, 131.84 (q, *J* = 32.9 Hz), 130.02 (d, *J* = 7.3 Hz), 129.47, 127.69, 124.89, 122.89 (q, *J* = 3.5 Hz), 122.52 (q, *J* =127.4 Hz), 121.16 (q, *J* = 3.8 Hz), 114.12, 111.69, 54.76, 45.75, 34.34. HRMS (ESI^-): m/z: 355.1082 $[M+H]^+$.

3-(Trifluoromethyl)phenyl isothiocyanate (0.63 mg, 3.08 mmol, 1 eqv) was dissolved in dichloromethane (30 mL), 2-phenylethyl amine (0.37 mg, 3.08 mmol, 1 eqv) was added, and then the reaction mixture was stirred for 2 h. The solvent was evaporated off by vacuum, and subsequently the residue was recrystallized from ethylacetate. A white solid (0.94 g, 94 %) was obtained as compound Y21. m.p. 96.2-96.7°C. ^{1}H NMR (300 MHz, Chloroform-*d*) δ 8.36 (s, 1H), 7.56 – 7.26 (m, 5H), 7.24 – 7.18 (m, 2H), 7.18 – 7.11 (m, 2H), 5.99 (s, 1H), 3.90 (q, *J* = 6.7 Hz, 2H), 2.93 (t, *J* = 6.7 Hz, 2H). ^{13}C NMR (75 MHz, $CDCl_3$) δ 180.19, 137.85, 136.56, 132.11 (q, *J* = 32.8 Hz), 130.22, 128.47, 128.30, 127.80, 126.46, 124.80, 123.16 (q, *J* = 7.4, 3.5 Hz), 121.32 (q, *J* = 3.7 Hz), 45.96, 34.31. HRMS (ESI^-): m/z: 325.0977 $[M+H]^+$.

The rest target compounds were synthesized using the same methodology, and the characterization data of ^{1}H NMR, ^{13}C NMR, HRMS, and melting point are shown below. The ^{1}H NMR and ^{13}C NMR spectra images can be found in the appendix.

Compound Y2, yellow liquid (0.93 g, 93 %), ^{1}H NMR (300 MHz, Chloroform-*d*) δ 8.01 (s, 1H), 7.29 – 7.19 (m, 2H), 7.08 (d, *J* = 1.7 Hz, 1H), 6.85 – 6.60 (m, 5H), 6.05 (s, 1H), 3.88 (q, *J* = 6.8 Hz,, 2H), 3.83 (s, 3H), 3.79 (s, 3H), 2.84 (t, *J* = 6.8 Hz, 2H), 1.24 (s, 9H). ^{13}C NMR (75 MHz, $CDCl_3$) δ 180.10, 153.46, 148.79, 147.42, 135.34, 130.58, 129.23, 123.89, 121.98, 121.68, 120.21, 111.49, 111.08, 55.55, 55.48, 46.02, 34.42, 34.08, 30.77. HRMS (ESI^-): m/z: 373.1944 $[M+H]^+$.

Compound Y3, yellow solid (0.95g, 95 %), m.p. 78.9- 80.6°C. ^{1}H NMR (300 MHz, Chloroform-*d*) δ 7.87 (s, 1H), 7.23 (t, *J* = 7.8 Hz, 1H), 7.10 (d, *J* = 7.8 Hz, 1H), 6.91 – 6.62 (m, 5H), 6.05 (s, 1H), 3.90 (q, *J* = 6.8 Hz,, 2H), 3.84 (s, 3H), 3.81 (s, 3H), 2.82 (m, 3H), 1.19 (s, 3H), 1.17 (s, 3H). ^{13}C NMR (75 MHz, $CDCl_3$) δ 179.98, 150.98, 148.79, 147.42, 135.63, 130.63, 129.50, 124.86, 122.76, 121.91, 120.23, 111.51, 111.07, 55.54, 55.48, 45.97, 34.04, 33.53, 23.39. HRMS (ESI^-): m/z: 359.1785 $[M+H]^+$.

Compound Y4, white solid (0.94 g, 94%), m.p. 124.5-125.2°C. ^{1}H NMR (300 MHz, Chloroform-*d*) δ 7.76 (s, 1H), 7.23 (t, *J* = 7.7 Hz, 1H), 7.08 (d, *J* = 8.0 Hz, 1H), 6.87 – 6.63 (m, 5H), 6.04 (s, 1H), 3.92 – 3.86 (m, 2H), 3.85 (s, 3H), 3.81 (s, 3H), 2.86 (t, *J* = 6.8 Hz, 2H), 2.57 (q, *J* = 7.6 Hz, 2H), 1.17 (t, *J* = 7.6 Hz, 3H). ^{13}C NMR (75 MHz, $CDCl_3$) δ 180.12, 148.83, 147.46, 146.39, 135.46, 130.62, 129.59, 126.48, 124.09, 121.86, 120.25, 111.51, 111.06, 55.57, 55.50, 46.06, 34.01, 28.21, 14.91. HRMS (ESI^-): m/z: 345.1628 $[M+H]^+$.

Compound Y5, white solid (0.94 g, 94%), m.p. 121.1-121.2°C. ^{1}H NMR (300 MHz, Chloroform-*d*) δ 7.68 (s, 1H), 7.26 – 7.18 (m, 1H), 7.07 (d, *J* = 7.7 Hz, 1H), 6.84 –

6.75 (m, 3H), 6.71 – 6.66 (m, 2H), 6.05 (s, 1H), 3.90 (q, *J* = 6.6 Hz,, 2H), 3.88 (s, 3H), 3.84 (s, 3H), 2.88 (t, *J* = 6.7 Hz, 2H), 2.29 (s, 3H). ^{13}C NMR (75 MHz, $CDCl_3$) δ 180.13, 148.85, 147.48, 140.04, 135.36, 130.63, 129.53, 127.69, 125.22, 121.65, 120.28, 111.52, 111.09, 55.59, 55.50, 46.06, 33.98, 20.86. HRMS (ESI^-): m/z: 331.1475 $[M+H]^+$.

Compound Y6, white solid (0.96 g, 96%), m.p. 128.3-128.4°C. ^{1}H NMR (300 MHz, Chloroform-*d*) δ 7.68 (s, 1H), 7.39 – 7.23 (m, 3H), 7.05 – 6.97 (m, 2H), 6.77 (d, *J* = 8.7 Hz, 1H), 6.71 – 6.64 (m, 2H), 6.02 (s, 1H), 3.90 (q, *J* = 6.7 Hz, 2H), 3.88 (s, 3H), 3.84 (s, 3H), 2.87 (t, *J* = 6.8 Hz, 2H). ^{13}C NMR (75 MHz, $CDCl_3$) δ 180.15, 148.85, 147.49, 135.43, 130.52, 129.78, 126.91, 124.72, 120.29, 111.47, 111.12, 55.64, 55.51, 46.11, 33.99. HRMS (ESI^-): m/z: 317.1315 $[M+H]^+$.

Compound Y7, white solid (0.95 g, 95%), m.p. 146.3 -147.1 °C. ^{1}H NMR (300 MHz, Chloroform-*d*) δ 8.59 (s, 1H), 7.27 – 7.20 (m, 1H), 6.89 (m, 1H), 6.83 – 6.73 (m, 3H), 6.66 (d, *J* = 6.9 Hz, 2H), 6.17 (s, 1H), 3.88 (q, *J* = 6.9 Hz,, 2H), 3.83 (s, 3H), 3.80 (s, 3H), 2.86 (t, *J* = 6.7 Hz, 2H). ^{13}C NMR (75 MHz, $CDCl_3$) δ 179.67, 162.80 (d, *J* = 248.9 Hz), 148.88, 147.54, 137.51 (d, *J* = 9.4 Hz), 130.82 (d, *J* = 9.3 Hz), 130.39, 120.31, 119.56 (d, *J* = 3.0 Hz), 113.21 (d, *J* = 20.9 Hz), 111.49, 111.42, 111.16 (d, *J* = 2.1 Hz), 55.56, 55.48, 45.93, 33.88. HRMS (ESI^-): m/z: 335.1224 $[M+H]^+$.

Compound Y8, yellow solid (0.92 g, 92%), m.p. 119.1-119.7°C. ^{1}H NMR (300 MHz, Chloroform-*d*) δ 7.88 (s, 1H), 7.25 – 7.18 (m, 2H), 7.05 (d, *J* = 2.0 Hz, 1H), 6.88 (m, 1H), 6.81 – 6.75 (m, 1H), 6.67 (d, *J* = 6.6 Hz, 2H), 6.02 (s, 1H), 3.89 (q, *J* = 6.9 Hz, 2H), 3.86 (s, 3H), 3.83 (s, 3H), 2.88 (t, *J* = 6.7 Hz, 2H). ^{13}C NMR (75 MHz,

242 $CDCl_3$) δ 180.01, 148.96, 147.61, 136.90, 135.25, 130.65, 130.34, 126.78, 124.52,
243 122.48, 120.29, 111.42, 111.15, 55.59, 55.53, 46.08, 33.89. HRMS (ESI^-): m/z:
244 351.0927 $[M+H]^+$.

245 Compound Y9, white solid (0.95 g, 95%), m.p. 136.5-137.6°C. ^1H NMR (300 MHz,
246 Chloroform-*d*) δ 7.98 (s, 1H), 7.36 (m, 1H), 7.24 – 7.13 (m, 2H), 6.94 (d, *J* = 8.1 Hz,
247 1H), 6.82 – 6.75 (m, 1H), 6.71 – 6.63 (m, 2H), 6.02 (s, 1H), 3.88 (q, *J* = 6.8 Hz, 2H),
248 3.86 (s, 3H), 3.83 (s, 3H), 2.87 (t, *J* = 6.7 Hz, 2H). ^{13}C NMR (75 MHz, $CDCl_3$) δ
249 180.00, 148.95, 147.59, 137.04, 130.88, 130.34, 129.72, 127.45, 123.09, 123.01,
250 120.29, 55.60, 55.54, 46.06, 33.89. HRMS (ESI^-): m/z: 395.0422 $[M+H]^+$.

251 Compound Y10, yellow solid (0.97 g, 97%), m.p. 146.5- 147.1°C. ^1H NMR (300
252 MHz, Chloroform-*d*) δ 7.91 (s, 1H), 7.57 (d, *J* = 7.6 Hz, 1H), 7.42 (s, 1H), 7.00 (m,
253 2H), 6.79 (d, *J* = 8.6 Hz, 1H), 6.71 – 6.64 (m, 2H), 5.99 (s, 1H), 3.89 (q, *J* = 6.7 Hz,,
254 2H), 3.86 (s, 3H), 3.83 (s, 3H), 2.87 (t, *J* = 6.7 Hz, 2H). ^{13}C NMR (75 MHz, $CDCl_3$) δ
255 179.99, 148.92, 147.56, 136.87, 135.77, 133.37, 130.99, 130.33, 123.79, 120.28,
256 111.39, 111.15, 94.56, 55.63, 55.56, 46.07, 33.90. HRMS (ESI^-): m/z: 443.0280
257 $[M+H]^+$.

258 Compound Y12, yellow liquid (0.94 g, 94%), ^1H NMR (300 MHz, DMSO-d_6) δ
259 8.08 (s, 1H), 7.31 – 7.08 (m, 4H), 6.87 – 6.66 (m, 4H), 6.04 (s, 1H), 3.89 (q, *J* = 6.6
260 Hz, 2H), 3.75 (s, 3H), 2.88 (t, *J* = 6.8 Hz, 2H), 1.26 (s, 9H). ^{13}C NMR (75 MHz,
261 $CDCl_3$) δ 180.16, 159.51, 153.46, 139.71, 135.27, 129.33, 129.25, 123.99, 122.09,
262 121.85, 120.59, 113.99, 111.70, 54.78, 45.88, 34.58, 34.44, 30.81. HRMS (ESI^-): m/z:
263 343.1835 $[M+H]^+$.

Compound Y13, brown solid (0.91 g, 91%), m.p. 59.8-61.0°C. ^{1}H NMR (300 MHz, DMSO-d_6) δ 8.06 (s, 1H), 7.26 – 7.07 (m, 3H), 6.91 (t, J = 2.0 Hz, 1H), 6.83 (d, J = 7.8 Hz, 1H), 6.77 – 6.68 (m, 3H), 6.05 (s, 1H), 3.89 (q, J = 6.7 Hz, 2H), 3.76 (s, 3H), 2.89 (t, J = 6.7 Hz, 2H), 2.85 – 2.77 (m, 1H), 1.20 (s, 3H), 1.18 (s, 3H). ^{13}C NMR (75 MHz, $CDCl_3$) δ 180.08, 159.53, 151.02, 139.76, 135.52, 129.56, 129.33, 124.97, 122.92, 122.09, 120.62, 114.02, 111.70, 54.78, 45.86, 34.54, 33.54, 23.43. HRMS (ESI$^-$): m/z: 329.1679 $[M+H]^+$.

Compound Y14, yellow solid (0.98 g, 98%), m.p. 58.9-60.1°C. ^{1}H NMR (300 MHz, DMSO-d_6) δ 8.10 (s, 1H), 7.26 – 7.02 (m, 3H), 6.90 – 6.67 (m, 5H), 6.06 (s, 1H), 3.88 (q, J = 6.6 Hz, 2H), 3.75 (s, 3H), 2.88 (t, J = 6.7 Hz, 2H), 2.57 (q, J = 7.6 Hz, 2H), 1.17 (t, J = 7.6 Hz, 3H). ^{13}C NMR (75 MHz, $CDCl_3$) δ 180.04, 159.53, 146.29, 139.79, 135.55, 129.56, 129.32, 126.39, 124.15, 121.94, 120.65, 114.04, 111.70, 54.79, 45.84, 34.52, 28.22, 14.95. HRMS (ESI$^-$): m/z: 315.1520 $[M+H]^+$.

Compound Y15, yellow solid (0.93 g, 93%), m.p. 94.6 -94.7°C. ^{1}H NMR (300 MHz, DMSO-d_6) δ 7.73 (s, 1H), 7.19 (m, 2H), 7.05 (d, J = 7.6 Hz, 1H), 6.85 – 6.67 (m, 5H), 6.02 (s, 1H), 3.90 (q, J = 6.6 Hz, 2H), 3.77 (s, 3H), 2.90 (t, J = 6.7 Hz, 2H), 2.28 (s, 3H). ^{13}C NMR (75 MHz, $CDCl_3$) δ 180.15, 159.55, 140.01, 139.79, 135.33, 129.54, 129.35, 127.71, 125.31, 121.75, 120.66, 114.05, 111.72, 54.79, 45.91, 34.49, 20.88. HRMS (ESI$^-$): m/z: 301.1363 $[M+H]^+$.

Compound Y16, yellow solid (0.92 g, 92%), m.p. 112.5-113.6°C. ^{1}H NMR (300 MHz, DMSO-d_6) δ 8.27 (s, 1H), 7.35 – 7.13 (m, 5H), 7.01 (d, J = 7.6 Hz, 1H), 6.78 – 6.66 (m, 3H), 6.04 (s, 1H), 3.88 (q, J = 6.8 Hz, 2H), 3.76 (s, 3H), 2.87 (t, J = 6.8 Hz,

2H). ^{13}C NMR (75 MHz, $CDCl_3$) δ 179.98, 159.55, 139.70, 135.62, 129.70, 129.40, 126.71, 124.70, 120.66, 114.07, 111.72, 54.82, 45.85, 34.50. HRMS (ESI^-): m/z: 287.1209 $[M+H]^+$.

Compound Y17, yellowish green solid (0.92 g, 92%), m.p. 74.2-75.0°C. ^{1}H NMR (300 MHz, DMSO-d_6) δ 8.26 (s, 1H), 7.31 – 7.15 (m, 2H), 6.92 (m, 1H), 6.74 (m, 5H), 6.09 (s, 1H), 3.90 (q, J = 6.9 Hz, 2H), 3.77 (s, 3H), 2.90 (t, J = 6.7 Hz, 2H). ^{13}C NMR (75 MHz, $CDCl_3$) δ 179.86, 162.88 (d, J = 249.1 Hz), 159.63, 139.54, 137.28 (d, J = 9.7 Hz), 130.92 (d, J = 9.1 Hz), 129.49, 120.61, 119.79 (d, J = 3.0 Hz), 114.15, 113.46 (d, J = 21.3 Hz), 111.72, 111.41, 54.80, 45.88, 34.33. HRMS (ESI^-): m/z: 305.1115 $[M+H]^+$.

Compound Y18, yellow liquid (0.97 g, 97%), ^{1}H NMR (300 MHz, DMSO-d_6) δ 8.23 (s, 1H), 7.25 – 7.16 (m, 3H), 7.08 (d, J = 2.1 Hz, 1H), 6.92 (m, 1H), 6.79 – 6.68 (m, 3H), 6.10 (s, 1H), 3.88 (q, J = 6.7 Hz, 2H), 3.77 (s, 3H), 2.90 (t, J = 6.7 Hz, 2H). ^{13}C NMR (75 MHz, $CDCl_3$) δ 180.00, 159.60, 139.56, 137.07, 135.15, 130.55, 129.48, 126.64, 124.52, 122.51, 120.63, 114.09, 111.78, 54.82, 45.89, 34.38. HRMS (ESI^-): m/z: 321.0821 $[M+H]^+$.

Compound Y19, yellow liquid (0.95 g, 95%), ^{1}H NMR (300 MHz, DMSO-d_6) δ 8.16 (s, 1H), 7.41 – 7.31 (m, 1H), 7.25 – 7.13 (m, 3H), 6.95 (d, J = 8.0 Hz, 1H), 6.81 – 6.68 (m, 3H), 6.02 (s, 1H), 3.89 (q, J = 6.5 Hz, 2H), 3.77 (s, 3H), 2.90 (t, J = 6.7 Hz, 2H). ^{13}C NMR (75 MHz, $CDCl_3$) δ 179.99, 159.61, 139.53, 137.06, 130.84, 129.72, 129.51, 127.53, 123.11, 123.09, 120.62, 114.07, 111.83, 54.84, 45.92, 34.37. HRMS (ESI^-): m/z: 365.0316 $[M+H]^+$.

Compound Y20, yellow liquid (0.96 g, 96%), ^{1}H NMR (300 MHz, DMSO-d_6) δ 8.06 (s, 1H), 7.57 (m, 1H), 7.43 (d, J = 1.5 Hz, 1H), 7.25 – 7.18 (m, 1H), 7.11 – 6.94 (m, 2H), 6.81 – 6.68 (m, 3H), 5.99 (s, 1H), 3.88 (q, J = 6.7 Hz, 2H), 3.78 (s, 3H), 2.90 (t, J = 6.7 Hz, 2H). ^{13}C NMR (75 MHz, $CDCl_3$) δ 180.02, 159.59, 139.54, 136.92, 135.75, 133.44, 130.94, 129.52, 123.91, 120.63, 114.05, 111.87, 94.57, 54.87, 45.92, 34.39. HRMS (ESI^-): m/z: 413.0172 $[M+H]^+$.

Compound Y22, white solid (0.93 g, 93%), m.p. 126.5 -127.0°C. ^{1}H NMR (300 MHz, Chloroform-*d*) δ 7.89 (s, 1H), 7.36 – 7.05 (m, 8H), 6.82 (d, J = 7.2 Hz, 1H), 6.00 (s, 1H), 3.90 (q, J = 6.5 Hz, 2H), 2.91 (t, J = 7.0 Hz, 2H), 1.26 (s, 9H). ^{13}C NMR (75 MHz, $CDCl_3$) δ 180.32, 153.53, 138.10, 135.19, 129.30, 128.34, 126.25, 124.12, 122.22, 121.98, 46.00, 34.54, 34.45, 30.82. HRMS (ESI^-): m/z: 313.1727 $[M+H]^+$.

Compound Y23, yellow solid (0.91 g, 92%), m.p. 77.5- 78.6°C. ^{1}H NMR (300 MHz, Chloroform-*d*) δ 7.86 (s, 1H), 7.30 – 7.08 (m, 7H), 6.90 (t, J = 2.0 Hz, 1H), 6.81 (m, 1H), 6.01 (s, 1H), 3.88 (q, J = 6.7 Hz, 2H), 2.91 (t, J = 6.8 Hz, 2H), 2.99 – 2.70 (m, 1H), 1.20 (s, 3H), 1.18 (s, 3H). ^{13}C NMR (75 MHz, $CDCl_3$) δ 180.22, 151.09, 138.15, 135.44, 129.60, 128.37, 128.34, 126.25, 125.09, 123.04, 122.20, 45.98, 34.49, 33.55, 23.43. HRMS (ESI^-): m/z: 299.1573 $[M+H]^+$.

Compound Y24, yellow solid (0.95 g, 95%), m.p. 71.0 -71.8°C. ^{1}H NMR (300 MHz, Chloroform-*d*) δ 8.10 (s, 1H), 7.30 – 7.10 (m, 6H), 7.07 (d, J = 7.7 Hz, 1H), 6.88 – 6.77 (m, 2H), 6.03 (s, 1H), 3.88 (q, J = 6.8 Hz, 2H), 2.91 (t, J = 6.8 Hz, 2H), 2.57 (q, J = 7.6 Hz, 2H), 1.17 (t, J = 7.6 Hz, 3H). ^{13}C NMR (75 MHz, $CDCl_3$) δ

180.05, 146.27, 138.20, 135.56, 129.58, 128.39, 128.34, 126.42, 126.26, 124.22, 122.00, 45.92, 34.48, 28.24, 14.98. HRMS (ESI$^-$): m/z: 285.1415 $[M+H]^+$.

Compound Y25, yellow solid (0.96 g, 96%), m.p. 92.4-93.3°C. ^{1}H NMR (300 MHz, Chloroform-*d*) δ 8.02 (s, 1H), 7.30 – 7.11 (m, 6H), 7.04 (d, *J* = 7.5 Hz, 1H), 6.80 (d, *J* = 7.6 Hz, 2H), 6.02 (s, 1H), 3.88 (q, *J* = 6.7 Hz, 2H), 2.91 (t, *J* = 6.8 Hz, 2H), 2.27 (s, 3H). ^{13}C NMR (75 MHz, $CDCl_3$) δ 180.08, 139.92, 138.20, 135.45, 129.52, 128.41, 128.35, 127.64, 126.27, 125.33, 121.77, 45.93, 34.45, 20.95. HRMS (ESI$^-$): m/z: 271.1259 $[M+H]^+$.

Compound Y26, yellow solid (0.94 g, 94%), m.p. 103.1- 109.7°C. ^{1}H NMR (300 MHz, Chloroform-*d*) δ 8.37 (s, 1H), 7.35 – 7.27 (m, 3H), 7.26 – 7.17 (m, 3H), 7.13 (m, 2H), 7.05 – 6.98 (m, 2H), 6.04 (s, 1H), 3.85 (q, *J* = 6.8 Hz, 2H), 2.90 (t, *J* = 6.8 Hz, 2H). ^{13}C NMR (75 MHz, $CDCl_3$) δ 179.96, 138.12, 135.72, 129.70, 128.41, 128.38, 126.67, 126.28, 124.71, 45.88, 34.47. HRMS (ESI$^-$): m/z: 257.1103 $[M+H]^+$.

Compound Y27, yellow solid (0.97 g, 97%), m.p. 79.9- 80. 8°C. ^{1}H NMR (300 MHz, Chloroform-*d*) δ 7.85 (s, 1H), 7.33 – 7.20 (m, 4H), 7.16 (m, 2H), 6.94 (m, 1H), 6.74 (m, 2H), 6.04 (s, 1H), 3.88 (q, *J* = 6.5 Hz, 2H), 2.94 (t, *J* = 6.8 Hz, 2H). ^{13}C NMR (75 MHz, $CDCl_3$) δ 179.87, 162.88 (d, *J* = 249.2 Hz), 137.94, 137.30 (d, *J* = 9.5 Hz), 130.94 (d, *J* = 9.3 Hz), 128.47, 128.37, 126.45, 119.79 (d, *J* = 3.0 Hz), 113.47 (d, *J* = 21.0 Hz), 111.60 (d, *J* = 23.4 Hz), 45.98, 34.33. HRMS (ESI$^-$): m/z: 275.1008 $[M+H]^+$.

Compound Y28, brownish yellow liquid (0.93 g, 93%), ^{1}H NMR (300 MHz, Chloroform-*d*) δ 8.15 (s, 1H), 7.36 – 7.29 (m, 2H), 7.26 – 7.06 (m, 7H), 6.92 (d, *J*=

6.5 Hz, 1H), 3.90 (t, *J* = 6.6 Hz, 2H), 2.94 (t, *J* = 6.5 Hz, 2H). ^{13}C NMR (75 MHz, $CDCl_3$) δ 137.97, 137.06, 135.15, 130.58, 128.48, 128.37, 126.69, 126.44, 124.61, 122.57, 46.15, 34.40. HRMS (ESI^-): m/z: 291.0714 $[M+H]^+$.

Compound Y29, yellow solid (0.95 g, 95%), m.p. 89.6- 90.0°C. ^{1}H NMR (300 MHz, Chloroform-*d*) δ 8.57 (s, 1H), 7.39 – 7.10 (m, 8H), 6.95 (m, 1H), 6.05 (s, 1H), 3.87 (q, *J* = 6.7 Hz, 2H), 2.91 (t, *J* = 6.8 Hz, 2H). ^{13}C NMR (75 MHz, $CDCl_3$) δ 179.85, 137.97, 137.23, 130.84, 129.60, 128.50, 128.38, 127.48, 126.46, 123.10, 123.00, 45.97, 34.39. HRMS (ESI^-): m/z: 335.0212 $[M+H]^+$.

Compound Y30, yellow solid (0.94 g, 94%), m.p. 86.7- 88.0°C. ^{1}H NMR (300 MHz, Chloroform-*d*) δ 8.38 (s, 1H), 7.62 – 7.41 (m, 2H), 7.34 – 6.94 (m, 7H), 6.00 (s, 1H), 3.87 (q, *J* = 6.5 Hz, 2H), 2.91 (t, *J* = 6.8 Hz, 2H). ^{13}C NMR (75 MHz, $CDCl_3$) δ 179.91, 137.97, 137.05, 135.67, 133.41, 130.95, 128.52, 128.38, 126.47, 123.93, 94.59, 46.00, 34.40. HRMS (ESI^-): m/z: 383.0073 $[M+H]^+$.

2.5. Biological assay

The biological activities of the synthesized compounds were assayed with the following procedures. [24, 25]

1/2 Murashige-Skoog (MS) culture medium, containing 0.8% agar, 1% sucrose, and the synthetic compounds with indicated concentration, was prepared and sterilized. *Arabidopsis* seeds including gibberellin-deficient dwarf mutant (*ga1-1*) and wild type *Arabidopsis* (Columbia-0, Col-0) were sterilized in 70% ethanol for 1 min and in 1% sodium hypochlorite solution for another 15 min, then were washed five times with sterile water, and grown on the 1/2 MS medium. Subsequently, the media were placed

in the illumination box at 22°C, after the *Arabidopsis* seeds were incubated at 4°C for 3 days. Hypocotyl length, taproot length, and root number of 7-day-old *Arabidopsis* seedlings were measured using ImageJ after image acquisition.

The rate of hypocotyl elongation was calculated based on the following equation:

$$P = \frac{L - L_0}{L_0} \times 100\%$$

where P is the rate of hypocotyl elongation increase, and L and L_0 are the average lengths of the Arabidopsis hypocotyl in the presence of the target compounds and in the control, respectively.

The inhibition rate of root growth was calculated according to the following equation:

$$I = \frac{d_0 - \mathrm{d}}{d_0} \times 100\%$$

where I is the inhibition rate, and d_0 and d are the average lengths of the Arabidopsis root in the control and in the presence of the target compounds, respectively.

2.6. Molecular dynamics simulation

Molecular dynamics simulation is a method for studying the interaction between ligand and target. The protonation states of histidine residues in the protein were manually inspected in order to ensure that all systems were optimized by the AMBER14 software. The force field parameters for protein were generated using AMBER ff99SB,[26] while those for ligands were generated by general AMBER force field (GAFF).[27] A rectangular water box filled with TIP3P water molecules with an edge of 12 Å was generated, and was used to fill the gaps between ligands and protein.

In addition, Na^+ ions were added to neutralize the system. This was followed by a 10 ns of production run of molecular dynamics simulations,[28] and the binding free energy was calculated using the MM/GBSA method.[29]

2.7. Molecular docking

Molecular docking was performed by the SYBYL 7.2 software using the Surflex-dock algorithm,[30,31] in which the crystal structure of GA_3-GID1A-DELLA from the RCSB protein data bank (PDB ID: 2ZSH) was used as the docking receptor. The receptor model was prepared by Biopolymer module, comprise Add MMFF94 charge, atom types of AMBER7 FF99, addition of hydrogen atoms and protonation states of amino acids were adjusted to pH 7.0. The optimal protocol in the active domain of the receptor was obtained using a ligand docking mode to improve docking accuracy. Unless otherwise indicated, all other parameters were defined as default values.

3. Results and discussion

3.1. Pharmacophore models and virtual screening

The GALAHAD module can accurately construct pharmacodynamics by using external macro definition files to specify overlapping features.[32] The pharmacophore characteristics produced by ligands are consistent with the crystal structure, and the additional pharmacophore characteristics help to enhance the affinity between ligands and target.[33] 20 pharmacophore models were established using the GALAHAD module and, a representative pharmacophore feature was selected from them (Fig. 3).

The enrichment factor (EF) of the pharmacophore model was 14.29 (Table S1), indicating that the model was reliable. The training set consisted of 200 active and non-active compounds.[34] The representative pharmacophore model comprised seven pharmacodynamic characteristics, which were mainly hydrophobic centers and acceptor atoms.

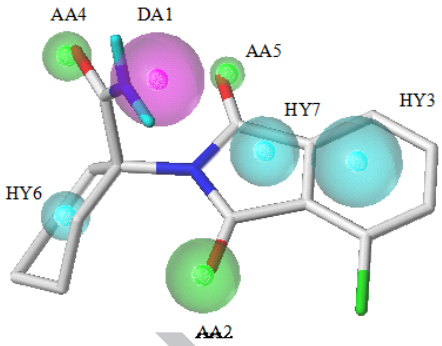

Fig. 3. The molecular alignment of the N-substituted phthalimide molecule AC94377 with its pharmacophore characteristics. Cyan spheres represent hydrophobic centers (HY), the magenta sphere represents the donor atom (DA), and green spheres represent acceptor atoms (AA).

Thiourea compounds were selected from the Maybridge database (Fig. S1). Initially, 7329 compounds were screened from the 56000 compounds of the Maybridge database through the Lipinski's rule of five and physicochemical properties. Subsequently, the aforementioned pharmacophore model was used to screen 3078 compounds, while target-based screening was also performed. Finally, 1-(2,3-dimethoxyphenethyl)-3-(3-(trifluoromethyl)phenyl)thiourea was selected based on their synthesizability, liposolubility, and water capacity as lead compounds, and subsequent design and synthesis was performed.

436

437 *3.2. Synthesis*

438 In general, amines and thiophosgene as beginning materials are usually used in the
439 synthesis of isothiocyanates due to the rapid reaction, ease in operation, and high yield.
440 However, thiophosgene is virulent. In this study, commercial available solid
441 dimethylamino thiocarbonyl chloride instead of thiophosgene was used with the same
442 features of ease operation, rapid reaction, and high yield. At the same time, it was
443 found that the substituents of aniline had little effect on isothiocyanate formation.
444 Since isothiocyanate is a reactive compound, the target compounds Y1-Y30 required
445 were prepared by only the mixing of the isothiocyanate with the amine. All target
446 compounds were characterized by ^{1}H NMR, ^{13}C NMR, and HRMS.

447

448 *3.3. Evalation of Biological activities of target compounds*

449 *3.3.1. Elongation effect of Arabidopsis hypocotyls*

450 In the bioassay, *Arabidopsis* was treated by all compounds (Y1-Y30) at
451 concentrations of 0.1, 1, 5, 10, 30 and 100 μmol/L in order to explore the multiple
452 effects of the synthetic compounds on *Arabidopsis* growth. The biological activities
453 results of compounds Y1-Y30 on *Arabidopsis* hypocotyl length (Columbia-0, Col-0)
454 are listed in Table 1. In total, most of the tested compounds had a promoting
455 elongation effect on Arabidopsis hypocotyl growth at 0.1, 1, and 10 μmol/L, and the
456 elongation increased with the increase of the concentration. However, the promoting
457 effect decreased, or turned to inhibition at 100 μmol/L. Among 30 compounds,

compound Y21 possesses the best promoting activity with hypocotyl elongation increase by 86.6% at 1 μmol/L, while the promotion effect of GA_3 was only 18.1% at the concentration. Thus, the promotion of hypocotyl elongation of compound Y21 was much better than that of gibberellin at low concentration. The overview of Arabidopsis growth treated with or without compound Y21 was showed in Fig. 4.

Table 1. Effect of compounds Y1-Y30 to hypocotyl length, taproot length, and root number of *Arabidopsis* (Columbia-0, Col-0)

Compd.	Concn. (μmol/L)	Enlongation rate (%)	Inhibition rate (%)	Root number	Compd.	Concn. (μmol/L)	Promoting rate (%)	Inhibition rate (%)	Root number
Y1	0.1	6.6±0.2	0.5±0.1	1	Y17	0.1	1.0±0.2	-0.1±0.2	2
	1	8.0±0.6	28.3±1.6	1		1	16.9±0.2	17.4±0.2	2
	10	118.1±1.3	50.3±3.3	2		10	16.3±0.2	42.7±0.2	3
	100	-21.8±0.3	94.7±2.5	1		100	93.5±0.2	90.4±0.2	1
Y2	0.1	1.5±0.7	2.8±0.4	1	Y18	0.1	0.0±0.1	1.2±0.4	1
	1	6.1±1.1	22.6±1.7	1		1	7.4±0.5	22.5±2.0	3
	10	68.1±3.2	51.2±1.9	3		10	22.7±1.3	48.9±3.8	3
	100	40.0±1.2	92.0±4.3	1		100	118.1±2.6	90.3±6.1	1
Y3	0.1	1.9±3.1	7.4±0.6	1	Y19	0.1	3.6±0.7	4.2±1.0	1
	1	29.2±0.9	21.1±0.5	1		1	28.5±2.9	31.6±2.3	3
	10	99.6±2.4	66.3±2.4	4		10	110.3±3.0	50.2±2.5	4
	100	67.9±0.2	91.4±3.8	1		100	96.8±5.1	90.7±4.6	1
Y4	0.1	1.0±0.4	10.7±1.4	1	Y20	0.1	0.9±0.3	14.2±1.4	1
	1	12.4±0.6	38.2±2.5	1		1	15.9±1.0	56.5±0.9	3
	10	106.9±0.5	38.6±0.9	3		10	79.3±0.8	67.8±1.7	3
	100	27.0±2.2	92.5±0.8	1		100	123.2±1.2	90.2±2.3	1
Y5	0.1	2.0±0.6	2.7±0.4	1	Y21	0.1	6.2±0.9	-19.0±1.9	3
	1	9.3±0.3	17.6±0.2	1		1	86.6±5.0	20.7±2.1	4
	10	34.7±1.1	24.1±1.6	1		10	29.8±3.6	76.5±2.2	2
	100	0.3±0.1	92.5±0.8	1		100	0.6±0.2	90.7±3.3	1
Y6	0.1	1.7±2.3	5.7±0.4	1	Y22	0.1	9.2±1.0	6.5±0.3	3
	1	3.6±0.8	6.1±3.7	1		1	22.1±0.6	70.5±1.9	3
	10	27.3±0.3	7.2±1.2	1		10	44.3±0.3	75.2±3.0	2
	100	-21.2±0.4	92.0±4.0	1		100	22.8±1.5	90.1±0.9	1
Y7	0.1	9.0±1.1	10.2±0.0	1	Y23	0.1	1.7±1.0	16.1±1.2	2
	1	20.2±1.0	11.8±0.7	1		1	14.6±2.6	58.4±3.8	4
	10	33.7±2.8	16.6±3.4	1		10	45.2±4.0	74.9±1.6	3
	100	22.9±2.1	91.4±2.6	1		100	-43.9±0.5	99.4±2.7	1

Y8	0.1	1.6±0.8	0.5±0.1	1	Y24	0.1	7.9±1.4	-6.1±0.1	1
	1	5.8±0.3	3.5±0.2	1		1	21.9±0.7	32.1±1.2	3
	10	39.7±1.2	48.7±2.4	1		10	53.1±2.0	69.5±0.4	3
	100	-31.4±1.4	97.2±5.2	1		100	-46.2±3.8	99.4±3.3	1
Y9	0.1	0.0±0.3	-34.7±0.5	1	Y25	0.1	1.1±0.5	2.5±0.1	1
	1	5.4±0.7	2.3±0.6	1		1	4.0±14	28.7±0.8	1
	10	18.2±1.0	35.9±2.0	3		10	44.5±2.6	58.7±2.3	2
	100	-30.9±1.1	98.2±6.5	1		100	-39.3±0.8	99.4±5.6	1
Y10	0.1	1.3±0.4	5.6±0.9	1	Y26	0.1	4.9±1.1	-1.0±0.2	1
	1	26.5±1.6	19.6±1.4	2		1	8.4±0.7	12.3±0.3	1
	10	50.7±2.3	60.9±2.6	2		10	9.0±1.6	34.7±0.7	1
	100	-4.5±1.8	93.7±0.7	1		100	7.9±0.5	90.4±3.2	1
Y11	0.1	1.5±0.5	21.4±0.5	1	Y27	0.1	4.0±0.1	13.4±0.8	1
	1	57.5±0.9	43.3±0.8	3		1	19.2±0.3	14.8±0.6	1
	10	97.7±1.3	78.1±0.4	3		10	12.3±0.9	35.4±2.8	2
	100	5.6±0.5	92.5±0.3	1		100	11.0±1.1	92.8±0.6	1
Y12	0.1	1.3±0.1	3.4±2.1	2	Y28	0.1	9.0±0.4	0.4±0.1	1
	1	36.4±1.0	40.7±1.8	3		1	20.3±0.6	-2.5±0.3	3
	10	68.8±2.1	59.5±1.6	4		10	55.9±3.5	34.9±2.4	3
	100	39.5±2.7	90.0±0.7	2		100	10.1±0.6	90.5±2.9	1
Y13	0.1	5.5±0.9	5.8±0.3	3	Y29	0.1	6.5±0.7	-0.1±0.2	1
	1	20.7±1.5	56.6±0.4	3		1	55.7±0.8	-2.5±0.8	3
	10	88.4±1.6	65.9±0.9	4		10	64.1±2.1	72.3±4.0	3
	100	18.0±0.2	90.4±3.0	1		100	-44.0±2.0	99.4±2.5	1
Y14	0.1	0.2±0.3	-1.5±0.2	3	Y30	0.1	0.4±0.1	26.1±0.2	2
	1	42.0±2.9	43.4±1.5	4		1	51.0±0.9	60.6±1.4	3
	10	77.4±2.6	65.1±2.4	4		10	68.0±3.5	80.0±0.9	1
	100	50.1±3.1	90.6±0.7	1		100	-53.4±0.6	99.4±1.7	1
Y15	0.1	1.2±0.4	5.2±0.1	2	GA_3	0.1	2.4±0.3	-3.7±0.5	1
	1	8.6±1.6	27.6±0.4	3		1	18.1±0.4	-1.6±0.1	1
	10	23.9±0.7	46.1±0.5	3		10	60.6±2.2	0±0.2	1
	100	18.8±0.9	90.3±2.6	1		100	123.5±0.9	8.6±0.5	1
Y16	0.1	0.0±0.2	5.6±0.8	1	DMSO	0.1	0.2±0.5	0.0±0.1	1
	1	9.6±0.6	16.4±2.9	1		1	0.2±0.4	0.7±0.2	1
	10	33.8±3.4	43.6±1.4	2		10	-2.2±0.0	1.9±0.7	1
	100	93.1±2.1	91.6±2.5	1		100	-3.6±0.6	12.7±0.4	1

In detail, most of the tested compounds, as well as GA_3, produced little effect on the growth of *Arabidopsis* hypocotyl at 0.1 μmol/L. At 1 μmol/L, the growth-promoting effect of several compounds, such as compounds Y3, Y10, Y11, Y21, Y29, and Y30 on *Arabidopsis* hypocotyls was greater than that achieved by the same concentration of GA_3. In particular, the promotion of compound Y21 was 4.8 times that of GA_3. At 10 μmol/L, the growth promoting effects of most compounds on *Arabidopsis* hypocotyls exceeded that of GA_3. For example, the hypocotyl length in *Arabidopsis* treated with compound Y1 at 10 μmol/L was 118% longer than that of the untreated ones, while the effect of GA_3 at the same concentration led to an only 73% elongation. However, when the concentration reached 100 μmol/L, the growth promoting effect of the tested compounds on *Arabidopsis* hypocotyl decreased, or turned to inhibition, which was consistent with the fact that plant growth regulators inhibit plant growth at high concentrations, but stimulate growth at lower concentrations.

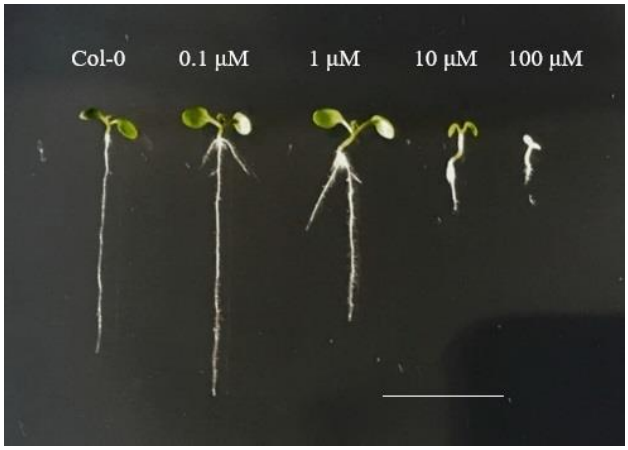

Fig. 4. The growth situation of 7-day-old *Arabidopsis* (Columbia-0, Col-0) seedlings, grown on 1/2 MS, containing 1% sucrose and 0.8% agar, either without or supplemented with compound

Y21 at the different indicated concentrations, bar = 5 mm.

Furthermore，it was noteworthy that the substituents on the phenyl and the number of methoxy groups on phenylethyl moiety of thiourea had a significant impact on hypocotyl elongation. For example, hypocotyl elongation was increased when R_1 (trifluoromethyl, chlorine, bromine or iodine) was an electron-withdrawing group and the number decrease of methoxy groups, and the elongation increase was tremendously improved from compound Y1 (8.0%, 1 μmol/L) to compound Y11 (57.5%, 1 μmol/L), and to compound Y21 (86.6%, 1 μmol/L). When R_1 was an electron-donating group, most of the compounds indicated that the reduction in the amount of the methoxy groups enhanced the bioactivities, and the complete disappearance of the methoxy groups weakened them.

At the same time, the electronic effect of substituents on the benzene ring affected bioactivity. When R_2, R_3 were methoxy, the activities of the compounds containing R_1 as an electron-donating group were much higher than those of the compounds containing R_1 as an electron-withdrawing group. For example, comparing compounds Y3 (99.6%, 10 μmol/L), and Y4 (106.9%, 10 μmol/L) with compounds Y7 (33.7%, 10 μmol/L) and Y8 (39.7%, 10 μmol/L), when R_2 was hydrogen and R_3 was hydrogen or methoxy, the activities of the compounds containing R_1 as an electron-withdrawing group were higher than those of the compounds containing R_1 as an electron-donating group.

Additionally, when the number of methoxy groups was constant, the promoting

activity of the compounds on *Arabidopsis* hypocotyls increased with the decrease of the electron donating ability and steric hindrance of group R_1. For instance, comparing compound Y2 (68.1%, 10 μmol/L) with compound Y3 (99.6%, 10 μmol/L), with compound Y4 (106.9%, 10 μmol/L). However, when R_1 was methyl or hydrogen, the activities of the compounds were dramatically decreased, and the order of activities of compounds substituted by electron-donating groups was obviously ethyl > isopropyl > *tert*-butyl > methyl > hydrogen. When R_1 was an electron-withdrawing group, the promoting activity of the compounds on *Arabidopsis* hypocotyl increased with the decrease of the electron-withdrawing ability. However, the trifluoromethyl group with higher steric hindrance did not follow the above laws, which led to higher activity. Thus, it was clear that the order of activities of compounds substituted by electron-donating groups was trifluoromethyl > iodium > bromo > chlorine > fluorine.

3.3.2. Evaluation of effect on Arabidopsis roots

While the synthetic compounds had an effect on *Arabidopsis* hypocotyl growth, they also had a significant effect on the growth of *Arabidopsis* roots, the IC_{50} values of Compounds Y1-Y30 to *Arabidopsis* taproot are shown in Table 2 and the numbers of the roots are shown in the Table 1. The results demonstrated that the synthetic compounds promoted or inhibited the growth of *Arabidopsis* taproots, and promoted the generation of *Arabidopsis* lateral roots. For example, compound Y21 promoted a taproot elongation of 19.0% at 0.1 μmol/L, while the IC_{50} values of compoundY21 to

529 *Arabidopsis* taproot is 6.3 μmol/L. At the same time, compound Y21 could effectively
530 increase the number of lateral roots to 3-4. The effect diagram of compound Y21 can
531 be seen in Fig. 4 and the biological activities results of compounds Y1-Y30 on taproot
532 length and root number of *Arabidopsis* are listed in Table 1.

533 In detail, it was observed that compounds Y9 and Y21 had a certain promoting
534 effect on the growth of *Arabidopsis* taproots at 0.1 μmol/L, with compound Y9
535 demonstrating the best promoting effect, reaching 34.7%. However, most of the
536 compounds inhibited *Arabidopsis* taproot growth, and it was found that the half
537 maximal inhibitory concentration values (Table 2) of the compounds with the best
538 inhibitory effect, such as compounds Y30, was 1.3 μmol/L. When the concentration
539 was 100 μmol/L, the inhibition rate of the tested compounds on taproot growth was
540 over 90%.

541

Table 2. The IC_{50} Values of Compounds Y1-Y30 to Arabidopsis Taproot

Compd	IC_{50} (μmol/L)	Compd	IC_{50} (μmol/L)	Compd	IC_{50} (μmol/L)
Y1	21.6	Y11	6.5	Y21	6.3
Y2	25.4	Y12	18.8	Y22	15
Y3	17.4	Y13	10.1	Y23	3.3
Y4	23.7	Y14	20.2	Y24	8.2
Y5	27.9	Y15	31.3	Y25	18.2
Y6	43.6	Y16	33.4	Y26	49.2
Y7	35.6	Y17	30.5	Y27	33
Y8	16.9	Y18	33.6	Y28	38.5
Y9	17	Y19	27.2	Y29	4.6
Y10	14.8	Y20	10.7	Y30	1.3

With the inhibition of taproot growth, the effect of the tested compounds on the number of lateral roots was also apparent. The root number of *Arabidopsis* treated with compounds Y13, Y14, Y21, and Y22 at 0.1 μmol/L was 3, and of the control was only 1. The root number of *Arabidopsis* treated with compounds Y14, Y21, and Y23 at 1 μmol/L was 4, and several compounds led to a root number of 3 and 2. The root number of *Arabidopsis* treated with compounds Y3, Y12, Y13, Y14, and Y19 at 10 μmol/L was 4, and several compounds led to a root number of 3 and 2. When the concentration was 100 μmol/L, the inhibition was too strong, which made the *Arabidopsis* roots to almost disappear and grow abnormally.

3.3.3. Evaluation of effect on Arabidopsis mutants

In addition, the gibberellin-deficient dwarf mutant (*ga1-1*) of *Arabidopsis* that could not grow normally without the application of exogenous GA, was also cultured in order to judge whether or not compound Y21 possessed a GA-like function of restoring mutant growth. The growth condition of the mutants can be seen in Fig. 5A and Fig. 5B. According to the results, it was observed that the 7-year-old mutant, treated without GA_3 or compound Y21, produced only short radicles and grew slowly, but after treated with GA_3 or compound Y21, it recovered its growth at different extent. As shown in Fig. 5A, the mutants treated with GA_3 at 10 and 100 μmol/L, grew well and its hypocotyl elongation was obvious, however, a weak root inhibition was observed at the concentration of 100 μmol/L. And the same biological activities

of compound Y21 on gal-1 were observed, too. By comparing Fig. 5A with Fig. 5B, it was found that compound Y21 produced better results than GA_3 at 0.1 and 1 μmol/L. More specifically, the hypocotyls were thicker, the lateral roots increased, and the root hairs were abundant. In total, the results demonstrated that compound Y21 displayed a GA-like function of restoring mutant growth.

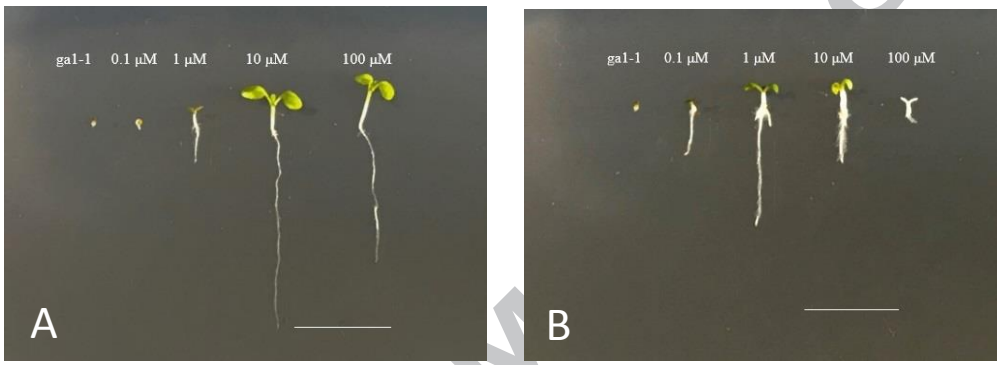

Fig. 5. The growth situation of 7-day-old gibberellin-deficient dwarf mutant (*ga1-1*) seedlings, grown on ½ MS, containing 1% sucrose and 0.8% agar, either without or supplemented with GA_3 (A) or compound Y21 (B) at the different indicated concentrations, bar = 5 mm.

3.4. Dynamical analysis and molecular docking

In order to study the affinity between three kinds of compounds and target protein, a complex system consisting of lead compounds Y1, Y11, and Y21 and the target protein was designed and used for dynamic simulation. The binding free energy calculation following a 10 ns molecular dynamic simulation (Fig. S2) of GA_3 and compounds Y1, Y11, and Y21 was performed using AMBER14. As it can be seen in Table 3, the affinity of compounds GA_3, Y1, Y11, and Y21 to target GID1A was -39.13, -46.91, -45.64, and -50.80, respectively. Apparently, the affinity of the

designed compounds to target GID1A was 1.2, 1.17, and 1.30 times stronger than that of GA_3, respectively. This could be possibly attributed to the polar interaction counteracts the electrostatic interaction. The results demonstrated that the designed compounds enhanced the affinity with the target, inducing higher biological activity at lower concentration. The biological activities of compounds Y1, Y11, and especially Y21 were better than those of GA_3. The important residues around the target active pockets provided similar van der Waals contributions to the four compounds, but the electrostatic interaction between the target protein and GA_3 was 1.25 and 1.34 times that between the designed synthetic compounds Y1 and Y11 and the target protein, respectively. In general, the designed and synthesized compounds reduced the adverse factors in the binding process with the target, thus enhancing the biological activity.

Table 3. The calculated binding free energy (kcal/mol) of the complex between different ligands and gibberellins receptor GID1A.

Energy Component	GA_3	Y1	Y11	Y21
ΔE_{VDW}	-44.42 ± 2.96	-47.79 ± 2.66	-43.83 ± 3.40	-42.67 ± 2.21
ΔE_{ele}	-33.02 ± 6.59	-26.51 ± 9.14	-24.71 ± 3.68	-30.37 ± 4.41
ΔG_{sol}	38.31 ± 3.53	27.39 ± 7.20	22.91 ± 2.55	22.23 ± 3.70
ΔG_{bind}	-39.13 ± 4.60	-46.91 ± 4.15	-45.64 ± 3.12	-50.80 ± 3.05

$\triangle E_{VDW}$,Van der Waals interaction.$\triangle E_{ele}$, Electrostatic interaction. $\triangle G_{sol}$: Polar interaction, $\triangle G_{bind}$, Binding free energy.

$\Delta G_{bind} = \Delta E_{VDW} + \Delta E_{ele} + \Delta G_{sol}$, value= Average ± std.

Molecular docking and binding free energy decomposition were performed in order to study the interaction patterns between the four compounds (GA_3, Y1, Y11, and Y21)

and the target. Murase et al. reported that residues, such as SER116, SER191, SER127, and ARG244, play an important role in the binding process between ligands and targets protein, but ASP190 exhibited a large polar interaction that hindered the binding,[10] which was well explained by molecular docking and free energy decomposition (Fig. S3, Table 4). These four compounds had similar binding patterns with target GID1A, and they could bind to important residues around the active pocket. ILE24, PHE27, and TYR31 were found to play important roles in the ligand, GID1A, and DELLA interactions in the lid region of the target. Compounds Y1, Y11 and Y21 were found to weaken polar interactions and collisions, while compound Y1 was found to weaken the polar interaction between GLY114 and ASP190. In addition, compounds Y11 and Y21 converted unfavorable residues GLY114 and ASP190 into contributing residues, thus enhancing their activity.

Table 4. Contribution rate (%) of some important residues to the ligand-target binding.

Residues	GA_3	Y1	Y11	Y21
ILE24	4.23	8.85	4.97	2.98
PHE27	13.09	11.05	9.34	6.21
TYR31	7.82	7.24	3.85	-2.44
GLY114	-2.03	-1.1	5.02	3.56
GLY115	1.49	1.82	4.95	2.79
SER116	3.55	3.58	6.02	2.3
HIS119	3.39	3.23	6.77	0.13
SER127	0.61	3.13	3.09	8.24
ASP190	-10.92	-4.74	9.22	1.4
SER191	8.42	1.95	6.19	9.38
VAL239	3.93	7.81	3.39	3.27
ARG244	8.19	15.65	2.66	0.7
VAL319	8.07	4.1	2.6	5.76
TYR322	3.82	1.31	2.38	6.08
LEU323	4.93	3.77	4.82	6.37

4. Conclusions

In summary, GID1A plays a critical role in GA biological identification and in the discovery of GAs functional analog, which makes it a promising drug action target. Combining structural information of GID1A and computer-aided technology, compound Y1, 1-(2,3-dimethoxyphenethyl)-3-(3-(trifluoromethyl)phenyl)thiourea was got from screening the Maybridge database, and twenty-nine analogues of Y1 were designed, synthesized and assayed *in vivo* in order to explore the GA-like compound. The bioassay results demonstrated compound Y21 is one of the most promising compounds, since it strongly promoted *Arabidopsis* hypocotyl elongation and root growth. In addition, the growth situation of *Arabidopsis* mutants indicated that compound Y21 has similar functions with GA_3. These observations suggest that compound Y21 is a candidate of promising plant growth regulator that provides a new insight into the molecular basis for future design and optimization of GA-like bio-regulators.

Acknowledgements

This research was supported by the National Key Research and Development Program of China (2017YFD0201300) and the Natural Science Foundation of China (31872850).

Declarations of interest

None.

Appendix A. Supplementary data

Supplementary data to this article can be found online.

References

1. Davies P J. Plant Hormones // Plant hormones. *Springer*. 2004.

2. Reinecke DM, Pharis RP. Gibberellin 3-oxidase gene expression patterns influence gibberellin biosynthesis, growth, and development in pea. *Plant Physiology*. 2013; 163:929-945.

3. Shani E, Weinstain R, Zhang Y, et al. Gibberellins accumulate in the elongating endodermal cells of Arabidopsis root. *Proceedings of the National Academy of Sciences of the United States of America*. 2013; 110:4834-4839.

4. Eugenio G Minguet，David Alabadí，Miguel A Blázquez. Gibberellin implication in plant growth and stress responses // Phytohormones: A Window to Metabolism, Signaling and Biotechnological Applications. *Springer*. 2014.

5. Petracek PD, Silverman FP. Greene DW. A History of Commercial Plant Growth Regulators in

Apple Production. *Hort-Science*. 2013; 38:937-942.

6. James M Hook, Lewis N Mander, Rudolf Urech. Total synthesis of gibberellic acid. The hydrofluorene route. *J Amer Chem Soc*.1980; 102:6628-6629.

7. Hou S, Zhu J, Ding M, et al. Simultaneous determination of gibberellic acid, indole-3-acetic acid and abscisic acid in wheat extracts by solid-phase extraction and liquid chromatography-electrospray tandem mass spectrometry. *Talanta*. 2008; 76:798-802.

8. M Ueguchi-Tanaka, M Ashikari, M Nakajima, et al. GIBBERELLIN INSENSITIVE DWARF1 encodes a soluble receptor for gibberellin. *Nature*. 2005; 437:693-8.

9. Nakajima M, Ashikari M, Takashi Y, et al. Identification and characterization of Arabidopsis gibberellin receptors. *The Plant Cell*. 2006; 46:880-889.

10. Murase K, Hirano Y, Sun T, et al. Gibberellin-Induced DELLA Recognition by the Gibberellin Receptor GID1. *Nature.* 2008; 456:459-464.

11. Shimada A, Ueguchi-Tanaka M, Nakatsu T, et al. Structural basis for gibberellin recognition by its receptor GID1. *Nature.* 2008; 456:520-523.

12. Fertel LB, O'Reilly NJ, Callaghan KM. Optimization of reaction variables in the selective hydrodechlorination of chlorinated phthalic anhydrides and acids: preparation of 3,6-dichlorophthalic acid and 3-chlorophthalic acid. *Cheminfor*. 1993; 58:261-263.

13. Suttle JC, Hultstrand JF. Physiological Studies of a Synthetic Gibberellin-Like Bioregulator: II. Effect of Site of Application on Biological Activity. *Plant Physiology*. 1987; 84:1068-1073.

14. Jiang K, Otani M, Shimotakahara H, et al. Substituted pthalimide AC94377 is a selective agonist of the gibberellin receptor GID1. *Plant Physiology*. 2016; 173:00937.

15. Gfeller D, Michielin O, Zoete V. Shaping the interaction landscape of bioactive molecules.

679 *Bioinformatics*. 2013; 29:3073-3079.

680 16. Friedrich C. Emil Fischer's Lock-and-Key Hypothesis after 100 years—Towards a
681 Supracellular Chemistry. *Perspectives in Supramolecular Chemistry: The Lock-and-Key*
682 *Principle, Volume 1*. 2007; 1-23.

683 17. Kuntz ID. Structure-based strategies for drug design and discovery. *Science*. 1992;
684 257:1078-1082.

685 18. Wlodawer A, Vondrasek J. Inhibitors of HIV-1 protease: A Major Success of Structure-assisted
686 Drug Design. *Annu Rev Biophys Biomol Struct*. 1998; 27:249-284.

687 19. Kryger G, Silman I, Sussman JL. Structure of Acetylcholinesterase Complexed with E2020:
688 Implications for the Design of New Anti-alzheimer Drugs. *Structure*. 1999; 7:297-307.

689 20. Sander T, Freyss J, Von KM, et al. Data Warrior: An open-source program for chemistry aware
690 data visualization and analysis. *J Chem Inf Model*. 2015; 55:460-473.

691 21. Kelder J, Grootenhuis PDJ, Bayada DM, et al. Ploemen JP. Polar molecular surface as a
692 dominating determinant for oral absorption and brain penetration of drugs. *Pharm Res*. 1999;
693 16:1514-1519.

694 22. Makarov VA, Braun H, Richter M, et al. Pyrazolopyrimidines: Potent Inhibitors Targeting the
695 Capsid of Rhino- and Enteroviruses. *Chemmedchem*. 2015, 10:1629-1634.

696 23. Busschaert N, Kirby IL, Young S, et al. Squaramides as potent transmembrane anion
697 transporters. *Angewandte Chemie*. 2012; 124:4502-4506.

698 24. Tian H, Xu Y, Liu S, et al. Synthesis of Gibberellic Acid Derivatives and Their Effects on Plant
699 Growth. *Molecules*. 2017; 22:694.

700 25. Liu S, Yu C, Tian H, et al. A Novel Bikinin Analogue for Arabidopsis, and Rice with Superior

Plant Growth-Promoting Activity. *J Plant Growth Regul.* 2017; 37:1-8.

26. Hornak V, Abel R, Okur A, et al. Comparison of multiple AMBER force fields and development of improved protein backbone parameters. *Proteins*. 2006; 65:712-725.

27. Wang J, Wolf RM, Caldwell JW, et al. Development and testing of a general AMBER force field. *J Comput Chem*. 2004; 25:1157-1174.

28. Chen X, Gan Q, Feng CG, et al. Virtual screening of novel and selective inhibitors of PTP1B over TCPTP using a bidentate inhibition strategy. *J Chem Inf Model*. 2018; 58:837-847.

29. Zhu YL, Beroza P, Artis DR. Including explicit water molecules as part of the protein structure in MM/PBSA calculations. *J Chem Inf Model*. 2014; 54:462-469.

30. Jain AN. Surflex: fully automatic flexible molecular docking using a molecular similarity-based a search engine. *J Med Chem*, 2003; 46:499-511.

31. Clark RD. Strizhey D. Leonard JM, et al. Consensus scoring for ligand/protein interactions. *J Mol Graphics Modell*. 2002; 20:281-295.

32. Abrahamian E, Fox PC, Naerum, L, et al. Efficient Generation, Storage, and Manipulation of Fully Flexible Pharmacophore Multiplets and Their Use in 3-D Similarity Searching. *J Chem In Comput Sci*. 2003; 43:458-468.

33. Richmond NJ, Abrams CA, Wolohan PR, et al. GALAHAD: 1. Pharmacophore Identification by Hypermolecular Alignment of Ligands in 3D. *J Comput Aid Mol Des*. 2006; 20:567-587.

34. Huang N, Shoichet BK, Irwin JJ. Benchmarking Sets for Molecular Docking. *J Med Chem*. 2006; 49:6789-6819.

Design, Synthesis, Biological Activities, and Dynamic Simulation Study of Novel Thiourea Derivatives with Gibberellin Activity towards *Arabidopsis thaliana*

Zhikun Yang[a, 1], Jine Wang[a, 1], Hao Tian[a], Yan He[a], Hongxia Duan[b], Liusheng Duan[a], Weiming Tan[a*]

[a] *College of Agronomy and Biotechnology, China Agricultural University, Beijing, 100193, P. R. China*

[b] *Department of Applied Chemistry, China Agricultural University, Beijing, 100193, P. R. China*